POLITECNICO DI TORINO
Repository ISTITUZIONALE

Enhanced electrochemical oxidation of phenol over manganese oxides under mild wet air oxidation conditions

Original
Enhanced electrochemical oxidation of phenol over manganese oxides under mild wet air oxidation conditions / Massa, Andrea; Hernández, Simelys; Ansaloni, Simone; Castellino, Micaela; Russo, Nunzio; Fino, Debora. - In: ELECTROCHIMICA ACTA. - ISSN 0013-4686. - ELETTRONICO. - 273:(2018), pp. 53-62. [10.1016/j.electacta.2018.03.178]

Availability:
This version is available at: 11583/2731036 since: 2019-04-16T23:06:18Z

Publisher:
Elsevier Ltd

Published
DOI:10.1016/j.electacta.2018.03.178

Terms of use:

This article is made available under terms and conditions as specified in the corresponding bibliographic description in the repository

Publisher copyright

(Article begins on next page)

27 April 2024

Electrochimica Acta 273 (2018) 53–62

Contents lists available at ScienceDirect

Electrochimica Acta

journal homepage: www.elsevier.com/locate/electacta

Enhanced electrochemical oxidation of phenol over manganese oxides under mild wet air oxidation conditions

Andrea Massa [a], Simelys Hernández [a, b, *], Simone Ansaloni [a], Micaela Castellino [b], Nunzio Russo [a], Debora Fino [a]

[a] CREST Group, Department of Applied Science and Technology, Politecnico di Torino, Corso Duca degli Abruzzi 24, 10129 Torino, Italy
[b] Center for Sustainable Future Technologies, IIT@Polito, Istituto Italiano di Tecnologia, corso Trento 21, 10129 Torino, Italy

ARTICLE INFO

Article history:
Received 15 January 2018
Received in revised form
25 March 2018
Accepted 28 March 2018
Available online 29 March 2018

Keywords:
Manganese oxide
Wastewater treatment
Phenol
Electro-oxidation
Catalytic wet air oxidation

ABSTRACT

Low-cost manganese oxide, MnOx-based electrocatalysts, containing α-MnO_2 and mixed α-Mn_2O_3/α-MnO_2 phases, were synthesized by scalable anodic and cathodic electrodeposition methods, respectively. Their morphological and chemical composition were characterized by means of Field Emission Scanning Electronic Microscopy (FESEM), X-Ray Diffraction (XRD) and X-ray Photoelectron Spectroscopy (XPS). These electrodes were tested for the electro-oxidation of a recalcitrant molecule (*i.e.* phenol) in a lab-scale high temperature and high pressure (HTHP) batch electrocatalytic reactor. Their electrocatalytic activity was compared with that of state-of-the-art anodes for phenol electro-oxidation: antimony-doped tin oxide (SnO_2—Sb^{5+}) and ruthenium oxide (RuO_2): first, under standard ambient conditions, and then, under the conditions of a Polymeric Electrolyte Membrane (PEM) electrolyzer (*i.e.* 85 °C and 30 bar) and of mild Catalytic Wet Air Oxidation (CWAO, *i.e.* 150 °C and 30 bar). Both reaction time and current density were varied to investigate their effect in the performances of the system as well as on the reaction mechanism. Both MnOx electrodes reported enhanced conversion efficiencies, up to ~75%, at the highest pressure and temperature, and at the lowest applied current density, which influenced the process by improving dissolution of the O_2 evolved, the reaction kinetics and thermodynamics, and by minimizing irreversibilities, respectively. The here reported MnO_x films achieved conversion and mineralization efficiencies comparable to *Sb-SnO₂* (that is the more toxic) and RuO_2 (that is more expensive) materials, operating under mild CWAO operation conditions, which demonstrate the potential of the electrocatalytic HTHP process as a sustainable advanced oxidation technology for wastewater treatment or electrosynthesis applications.

© 2018 The Authors. Published by Elsevier Ltd. This is an open access article under the CC BY-NC-ND license (http://creativecommons.org/licenses/by-nc-nd/4.0/).

1. Introduction

Water is the most important resource that has to be preserved and reutilized whenever possible. An important issue concerns the depuration of industrial wastewater, mainly containing either heavy metals or recalcitrant organics. Among the latter type of compounds, phenol and its derivatives are certainly the most problematic, due to their refractoriness to biological treatments, their high stability and their elevated toxicity even at low concentrations. Many efficient ways to treat these species have been employed in the last decades, especially methods belonging to the so-called advanced oxidation processes (AOPs), such as fenton and photo-fenton reactions [1], ozonation [2], wet air oxidation (WAO) [3], catalytic wet hydrogen peroxide oxidation (CWHPO) [4], and catalytic wet air oxidation (CWAO) [5]. Electrochemical degradation is another attractive procedure that has been considered to remove recalcitrant organics from water, especially in low-volume applications, due to its intrinsic high efficiency [6,7]. In addition, electrochemical systems could overcome some of the drawbacks of the abovementioned conventional catalytic processes because: earth abundant and no toxic catalysts can be used and expensive separation processes for catalyst recovery can be avoided [8]. Moreover, in electrochemical reactors, both reaction rate and selectivity could be easily tuned by simply modifying the applied current or electrode potential.

Abbreviations: HTHP, high-temperature and high-pressure; PEM, polymer electrolyte membrane; TOC, total organic carbon; CWAO, Catalytic Wet Air Oxidation.

* Corresponding author. CREST group, Department of Applied Science and Technology, Politecnico di Torino, Corso Duca degli Abruzzi 24, 10129 Torino, Italy.
E-mail address: simelys.hernandez@polito.it (S. Hernández).

https://doi.org/10.1016/j.electacta.2018.03.178
0013-4686/© 2018 The Authors. Published by Elsevier Ltd. This is an open access article under the CC BY-NC-ND license (http://creativecommons.org/licenses/by-nc-nd/4.0/).

Manganese oxides have been employed extensively in electrochemistry as cathodes in alkaline batteries, in lithium-ion batteries [9] and as pseudo-capacitive electrodes into supercapacitors [10–12], or as anodes for the water oxidation reaction [13,14]. The main advantages of manganese oxides are their low cost, if compared to Pt, IrO_2, RuO_2 and boron-doped diamond (BDD), and their lower toxicity than Sb-SnO_2 and PbO_2 [15–17]. In our previous work, different manganese oxide-based electrocatalyst supported on Ti foil were evaluated for the electro-oxidation of phenol, under ambient temperature and pressure conditions [18]. In particular, two kinds of electrodeposited films showed the highest activity and stability: an anodically electro-deposited sample and a cathodically electro-deposited film.

In this paper, a novel approach for the electrochemical treatment of wastewater containing recalcitrant organics is proposed. Phenol was used as target molecule, due to its stability and representativeness of refractory organic compounds. The adoption of high temperature and high pressure, up to mild Catalytic Wet Air Oxidation (CWAO) conditions, during the electrochemical process is expected to increase the efficiency of phenol removal and the degree of mineralization, due to the improved exploitation of the current provided to the system. Indeed, in the traditional direct electro-oxidation processes at ambient conditions, only highly reactive species such as hydroxyl radicals can degrade the organic compounds, whereas the oxygen, which is inevitably produced, is wasted as a by-product, thus lowering the faradic efficiency. Instead, under the here reported CWAO conditions, the in-situ electro-generated oxygen could be exploited for the degradation of phenol. Indeed, the increased pressure would improve the dissolution of O_2 in the aqueous matrix, which is expected to produce a decrease of the cell potential for the reaction [18].

The use of high temperature and pressure in electrochemical systems has been largely employed for electrochemical H_2 production, especially for alkaline electrolysis [19,20], and its beneficial effects on thermodynamics of the water splitting process has already been demonstrated [21–23]. The novel aspect of this work is the application and the analysis of operative conditions different from ambient temperature and pressure to electrochemically remove recalcitrant organics from wastewater, also adopting easily scalable and low-cost electro-catalysts. Therefore, the performances of manganese oxide electrodes were compared with two of the most performing types of anode used for this application [24–26]: electrodeposited antimony-doped tin oxide (SnO_2-Sb^{5+}) film and thermally deposited ruthenium oxide (RuO_2), both deposited in the same titanium foil used for the MnO_x samples for a proper comparison. The morphology, crystalline structure and superficial chemical composition of all the electrodes were investigated by means of field emission scanning electronic microscopy (FESEM), X-Ray diffraction (XRD) and X-ray photoelectron spectroscopy (XPS). Their electrocatalytic activity was first evaluated under ambient conditions, for comparison under commonly used standard conditions, and then, under PEM electrolyzer conditions (*i.e.* 85 °C and 30 bar) and mild Catalytic Wet Air Oxidation (CWAO) conditions (*i.e.* 150 °C and 30 bar). Moreover, the role of both reaction time and current density in the performances of the system were systematically investigated and correlated with the products distribution and mechanism of reaction on each investigated electrode material.

2. Experimental

2.1. Ti substrate preparation

Titanium foils (Sigma-Aldrich, 99.7%, thickness 250 μm) were pretreated according to the following procedure [18]: foils were polished with 320-grit sandpaper, then ultrasound cleaned in 2-propanol for 15 min to remove sandblasting grit [27]. A degreasing in 40% NaOH at 50 °C for 20 min was carried out to eliminate organic deposits. Shortly before the electro-deposition the substrate was etched for 1 min in HF solution (1.2% w/w) to remove the native oxide layer.

2.2. MnO_x electrodes synthesis

Electrodeposition of manganese oxides was carried out by following our previously reported method [18], by setting the Ti foil as the anode, a Pt wire as the cathode and an Ag/AgCl 3 M KCl (+0.209 V vs NHE) as the reference electrode. The anodically deposited sample (*i.e. An-MnO_x*) was prepared by dipping the titanium foil in a solution containing 0.1 M of $Mn(CH_3COO)_2$ as Mn precursor and 0.1 M Na_2SO_4 as supporting electrolyte. A current density of 2.5 mA/cm^2 was applied to the system for 10 min. The cathodically deposited sample (*i.e. Cat-MnO_x*) was synthesized by dipping the Ti foil in 150 ml of 0.01 M of $KMnO_4$ and 0.1 M Na_2SO_4 solution and applying a current density of −2.5 mA/cm^2 for 10 min. Both the samples were calcined in a muffle oven at 500 °C for 1 h, with a temperature ramp of 20 °C/min, to obtain different crystalline structures.

2.3. SnO_2–Sb^{5+} electrodes synthesis

The synthesis of the antimony-doped tin oxide films was carried out with an electro-deposition procedure described elsewhere [28]. The Ti foil was alternatively dipped in precursor solutions of $SbCl_3$ (Fluka, > 99.0%) and $SnCl_4 \cdot 5H_2O$ (Fluka, 98.0%). Sb^{3+} ions were first electrodeposited on the Ti substrate in a solution containing 0.01 M of $SbCl_3$ and 0.05 M citric acid (Sigma Aldrich, 99%) for 1 min at a constant current density of −2 mA/cm^2. After rinsing with DI water, the electrode was then dipped in a solution containing 0.1 M of $SnCl_4$ and 0.05 M H_2SO_4 (Fluka, 95–98%), and a current density of −2 mA/cm^2 was applied for 25 min. This procedure was repeated for 2 times to obtain a layer-by-layer electrodeposited material. The sample was then rinsed and left to dry in air. Finally, the electrode was annealed in a muffle oven at 550 °C for 6 h, with a calcination ramp of 20 °C/min.

2.4. RuO_2 electrodes synthesis

The film of ruthenium oxide was obtained via a thermal deposition method reported elsewhere [29]. The precursor solution was 0.1 M $RuCl_3 \cdot xH_2O$ (Sigma Aldrich, 38–42% Ru basis) dissolved in 2-propanol (Sigma Aldrich, 99.5%), with the addition of some drops of HCl (Fluka, 37%). The solution was applied to the surface of the Ti foil by brush coating, dried at 80 °C in air for 10 min, and then calcined in a muffle oven at 500 °C for 15 min. The procedure was repeated 10 times. Finally, the sample was annealed at 500 °C in air for 2 h.

2.5. Physico-chemical characterization of the electrodes

The structure, morphology and physical-chemical characteristics of the electrodes were assessed by X-Ray diffraction (XRD, X'Pert PRO diffractometer, Cu Kα radiation $\lambda = 1.54$ Å), X-ray photoelectron spectroscopy (XPS, PHI5000 VersaProbe) and field emission scanning electronic microscopy (FESEM, Zeiss Merlin). The loading of the coatings on the electrodes was measured by using a microbalance (Mettler Toledo UMX2, with 0.1 μg of resolution) after the deposition.

2.6. Electro-oxidation tests

All the synthesized samples were tested in different conditions: a first screening set of tests was carried out in a beaker at ambient conditions, then high temperature and pressure experiments were carried out in the HTHP reactor.

2.6.1. Electro-oxidation tests at ambient conditions

Firstly, all the electrodes were tested on a small scale (1 cm^2) in standard El-Ox conditions (*i.e.* at ambient temperature and pressure). Experiments were carried out in an undivided and unstirred glass cell containing 15 ml of a phenol solution ($C_0 = 100$ mg/l) and 0.1 M Na_2SO_4 as supporting electrolyte. The samples were used as anode, while Pt wire was set as cathode. A constant current density of 2.5 mA/cm^2 was applied to the system for 5 h. This value is far lower than those commonly used in literature (around 10–20 mA/cm^2). It was chosen since it is the minimum theoretical current needed to completely oxidize phenol, according to Eq. (1) and Eq. (2):

$$C_6H_6O + 7O_2 \rightarrow 6CO_2 + 3H_2O \quad \left(28e^-\right) \tag{1}$$

$$i = \frac{I}{A_{el}} = \frac{z \cdot F \cdot \frac{C_{0_{phenol}}}{PM_{phenol}} \cdot V_{sol}}{\Delta t \cdot A_{el}} \tag{2}$$

where I is the electro-oxidation current, A_{el} is the area of the electrode (1 cm^2), Δt is the electro-oxidation time (5 h), z is the number of electrons involved (28), F is Faraday's constant (96487 C/mol), C_0 is the initial phenol concentration (100 mg/l), PM_{phenol} is the molecular weight of phenol (94 g/mol) and V_{sol} is the volume of the solution (15 ml). The resulting value (*i.e.* 2.4 mA/cm^2) was approximated to 2.50 mA/cm^2. Thus, the total organic carbon (TOC) conversion coincides with the faradaic efficiency (FE), which is defined as:

$$FE = \frac{TOC_{fin} - TOC_{in}}{\Delta TOC_{theor}} \tag{3}$$

where TOC_{fin} and TOC_{in} are the final and initial measured values of TOC (g/l), while ΔTOC_{theor} is the theoretical variation of TOC, and it is equal to 72 g/l, as the current density is set to obtain a final theoretical value of TOC equal to zero. Higher current densities could have been applied, but this was not implemented since the reaction overpotential would have reached higher values, thus decreasing the faradaic efficiency of the process.

2.6.2. Electro-oxidation tests in the high-temperature high-pressure (HTHP) reactor

The electro-degradation tests under mild HTHP conditions were carried out in a home-made reactor. This lab-scale batch reactor consists of two separated chambers (500 ml each), where anodic and cathodic reactions take place. A pipe connects the two compartments, where a membrane can eventually be placed. The equipment is made of AISI 316 stainless steel and it can resist up to 50 bars and 200 °C. A hotplate with magnetic stirrer provides both the heat and continuous mixing. Temperature and pressure sensors are placed on the top of the chambers. The tests were made by using liquid batch conditions.

Subsequently, the synthesized electrodes (40 cm^2) were used as anodes for the electro-oxidation (El-Ox) of phenol and a Pt foil (~15 cm^2) was employed as the cathode. No reference electrode and membrane were utilized. Different test conditions were used: 85 °C and 30 bar, *i.e.* similar to some PEM electrolysis conditions [30], and 150 °C and 30 bar, which are comparable to mild CWAO conditions [31].

For both the experiments, the electric charge that passed through the system was set at the minimum required for the complete mineralization of phenol, which was 800 mA h (q), calculated by Eq. (4):

$$q = I \cdot \Delta t = z \cdot F \cdot \frac{C_{0_{phenol}}}{PM_{phenol}} \cdot V_{sol} \tag{4}$$

where C_0 is 100 mg/l and V_{sol} is 1 l.

2.7. Accelerated life-time tests

The durability of the synthesized electrodes was assessed through accelerated lifetime tests carried out in an unstirred and undivided glass cell, containing 15 ml of a 1 M Na_2SO_4 aqueous solution. Pt wire was used as the cathode and Ag/AgCl, 3 M KCl (+0.209 V vs NHE) as the reference electrode. A current density of 100 mA/cm^2 was applied to the cell. The electrode was considered deactivated when the measured potential reached 10 V.

2.8. Ohmic drop compensation

A preliminary characterization of the reactor by Electrochemical Impedance Spectroscopy (EIS) was performed to evaluate the ohmic drop of the system during the tests and to compensate the cell potential. The EIS measurements were carried out by using two Pt electrodes. The resistance of the solution was determined at a cell potential of 4.5 V, which is commonly reached in electro-oxidation treatments [32], and by setting an alternate current (AC) frequency of 10^5 Hz.

2.9. Analytical methods

High-performance liquid chromatography (HPLC Prominence by Shimadzu, with a Diode Array Detector DAD set at 206 nm) and Total Organic Carbon (TOC-V_{CPH} Carbon Analyzer by Shimadzu) analyses were performed on the treated solutions (stored under ambient conditions) to determine the percentage of phenol degradation and mineralization, respectively. The HPLC instrument was equipped with a Phenomenex Rezex ROA organic acids H^+ column (300 × 7.8 mm) operating at 333 K, while the eluent was 5 mM H_2SO_4 in water at 0.6 ml/min of flow speed. HPLC was also used to determine the intermediate compounds formed during the degradation, with the different electrode materials, to compare the reaction pathways with the ones presented in literature. The chromatograms of all the compounds and their retention times (t_R), which were identified by using internal standards, are shown in Fig. S1 of the Supplementary Information (SI). It is worth mentioning that no detailed quantitative analysis of the intermediates was made in this case, as their concentrations were estimated to be around 1–2 ppm each, or even less.

3. Results and discussion

3.1. XRD analysis

Fig. 1 shows the XRD patterns for all the synthesized electrodes, in comparison with the XRD spectrum of the bare Ti foil used as substrate. As expected, Ti foil showed only the peaks related to metallic Ti (Fig. 1a). The *An-MnO_x* sample (Fig. 1b) evidenced two

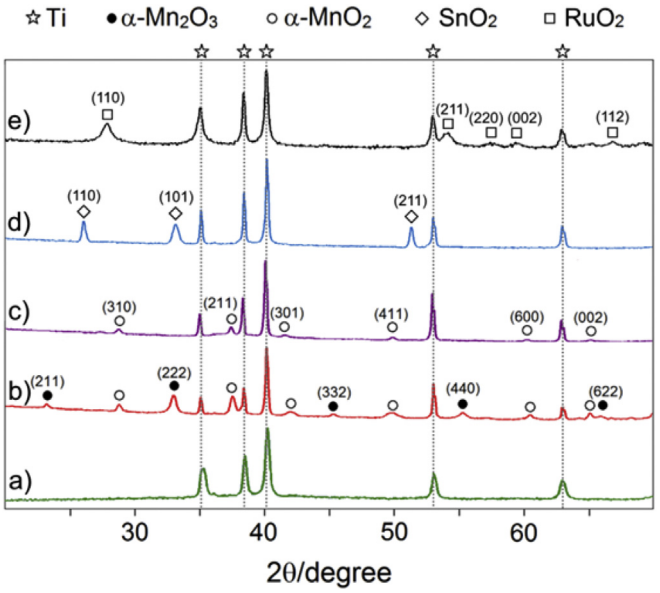

Fig. 1. XRD patterns of deposited metal oxide films on Ti: (a) Ti, (b) An-MnO_x, (c) Cat-MnO_x, (d) SnO_2-Sb and (e) RuO_2.

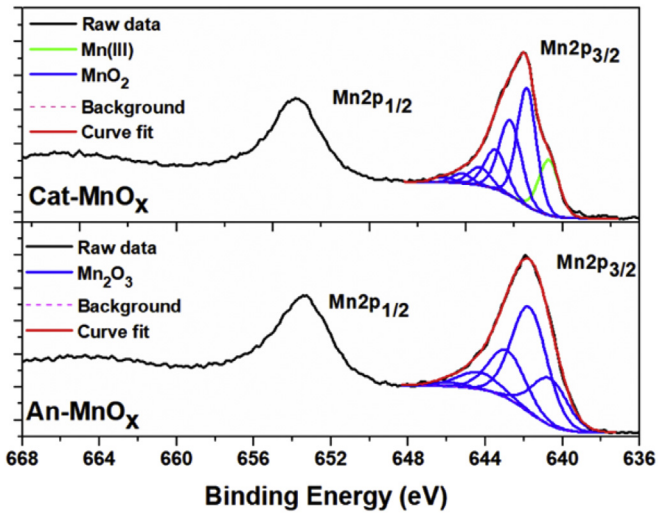

Fig. 2. XPS Mn2p high resolution spectra for *Cat-MnO_x* (top) and *An-MnO_x* (bottom) samples.

different MnO_x crystalline phases: a cubic bixbyite α-Mn_2O_3 phase and a tetragonal manganese dioxide α-MnO_2 phase (JCPDS 041-1442, Ia−3, a = 0.941 nm; JCPDS 044-014, *I*4/*m*, a = b = 9.7847, c = 2.8630) [18]. Instead, in the *Cat-MnO_x* sample (Fig. 1c), only the XRD pattern of the tetragonal α-MnO_2 (JCPDS 044-014, *I*4/*m*, a = b = 9.7847, c = 2.8630) was detected [18]. For the SnO_2-Sb film (Fig. 1d), three main peaks were observed at 26.2°, 33.5° and 51.6°, which are attributable to a tetragonal tin oxide phase (JCPDS 001-0625, *P*42/*mnm*, a = b = 4.7200, c = 3.1700), whereas the antimony peaks were not detected due to its low concentration in the film. The RuO_2 sample (Fig. 1e) showed the typical XRD pattern of the tetragonal ruthenium oxide (JCPDS 040-1290, *P*42/*mnm*, a = b = 4.4994, c = 3.1071), even though some of the main peaks at 35.1° and 40.0° are covered by the peaks of Ti.

3.2. XPS analysis

XPS analysis was performed in order to obtain information regarding the Mn oxidation states for both the *An-MnO_x* and Cat-MnO_x samples. It is well-known in literature that fitting the Mn2p doublet to obtain information regarding the MnO_x species represents a challenge. This is because Mn possesses six stable oxidation states, three oxidation states with significant multiplet splitting (II, III, IV) and complex overlapping binding energy ranges. In this work, a method described elsewhere [33] was used to fit the Mn2p XPS spectra of the two MnOx samples. For the sake of simplicity only the $Mn2p_{3/2}$ peak has been deconvoluted as reported in Fig. 2. The *An-MnO_x* sample was deconvoluted with 5 curves, all due to the Mn^{+3} oxidation state [33] corresponding to the Mn_2O_3, in agreement with the XRD data. Instead, the Cat-MnO_x sample has required 7 curves to overlap the raw data curve. The first component at 640.7 eV that could be attributed to some $Mn^{+3,}$ while the remaining 6 are all due to the Mn^{+4} state for MnO_2, which was the main crystalline phase found for this sample in the XRD spectrum. The Mn^{+3} amount was determined to be of about 17% of the total Mn signal, in accordance with the reported values for pyrolusite (a MnO_2 mineral). The absence of the shake-up feature at binding energies higher than 645 eV, for both the samples, is a clue that no Mn^{+2} is present.

3.3. FESEM analysis

Fig. 3 shows the FESEM images of the electrocatalytic films. The insets highlight the details of the morphologies, while the lower magnification images gave an overview of the Ti covered by the electrocatalytic layers. Fig. 3a shows the structure of the anodic sample (*i.e. An-MnO_x*), which is constituted by large crystalline nanoparticles, together with very fine nanoflakes. Such a coexistence of different morphologies could be explained by the two MnO_x phases present in this sample, as demonstrated by the XRD spectra: α-Mn_2O_3 and α-MnO_2. In fact, they have different crystalline organization, which lead to the formation of a non-homogeneous structure of the film. The morphology of the cathodic sample (*Cat-MnO_x*) shown in Fig. 3b is characterized by nanoflakes forming a layer directly over the Ti foil, from which large polycrystalline rod-like structures grew up. The *SnO_2-Sb* anode in Fig. 3c, shows a cracked-mud morphology probably due to the calcination, which is even more evident due to the very fine nanocrystalline structure of the layer as shown in the inset of Fig. 3c. Fig. 3d shows the FESEM images of the thermally deposited *RuO_2* anode, which presents large crystalline nanoparticles uniformly spread over the electro-catalytic film.

3.4. Ohmic drop analysis

Results of the tests carried out in the HTHP reactor at different conditions showed that the initial solution (1 l of 100 mg/l phenol and 0.1 M Na_2SO_4), with at a distance of ~10 cm between anode and cathode, had ohmic resistances between 21.2 Ω at ambient conditions and 9.9 Ω at 150 °C and 30 bar. As expected, a strong influence of the temperature on the conductivity of the solution was clearly evidenced [19], as shown in the Supporting Information (Fig. S2). The strong effect of the temperature is easily explained by the enhanced ion mobility, and due to the drop in the solution viscosity.

Surprisingly, the pressure increase determined a slight decrease in the electrolyte resistance, especially in the range from 5 to 10 bar, where the decrease was more pronounced than in the range 10−30 bar. At such low pressures, the effect of the rise in the liquid viscosity could be neglected. Hence, most probably this effect was due to two phenomena [34]:

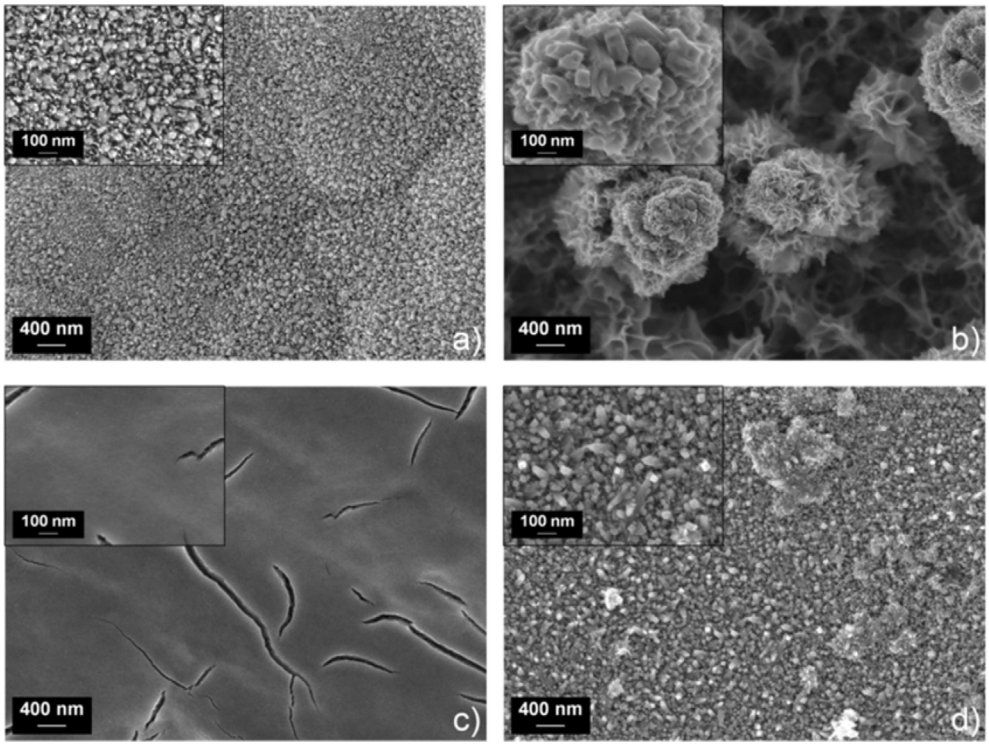

Fig. 3. FESEM images of deposited metal oxide films on Ti: (a) An-MnO_x, (b) Cat-MnO_x, (c) SnO_2-Sb and (d) RuO_2.

1) the increase of the pressure partially compressed the volume of the solution, which slightly increased the concentration of the electrolyte (Na_2SO_4). However, this enhancement should account only for a part of the total effect;
2) the change in the dissociation equilibrium of sodium sulfate could have improved the amount of Na^+ and SO_4^{2-} ions in the solution;

The electrolyte resistance at 25 °C was lower in the HTHP reactor than in the beaker, even though the distance between the electrodes was higher in the HTHP reactor. Since the electrolyte solution was the same and hence the resistivity (ρ, $\Omega \cdot m$) was unvaried, this phenomenon could be explained because of the different geometry of the test units. According to Eq. (5), since the electrode area (A, m^2) used in the HTHP reactor was higher than that used in the beaker, this compensated the higher distance between the electrodes (l, m) in the former system.

$$R_s = \rho \cdot \frac{l}{A} \tag{5}$$

3.5. Standard electro-oxidation tests under ambient conditions

Fig. 4 shows the performances under ambient conditions of the synthesized electrocatalysts. The *An-MnO_x* sample, which was obtained by anodic deposition is constituted by α-Mn_2O_3/α-MnO_2, showed the lowest electro-degradation efficiency of phenol (22.3%) under these tests conditions, with a poor degree of mineralization, as indicated by the TOC analysis (11.3%). This behavior was most probably due to the presence of the α-Mn_2O_3 phase in this sample, which is known to have a low overpotential for the water splitting reaction [15,35–37]. As a consequence, a large part of the current provided to the system was most probably used for the oxygen evolution reaction.

On the contrary, with the *Cat-MnO_x* sample, which was synthesized by cathodic electro-deposition, the overall phenol abatement and TOC reduction were greatly improved up to 42.7% and 27.6%, respectively, thus doubling the efficiencies obtained in the tests with the anodic sample. This trend is reasonably explained by the composition of the *Cat-MnO_x*, which contains principally α-MnO_2 that is considered as the most active MnO_x phase for the electro-oxidation of organic compounds [38,39].

The two "reference" anodes (*i.e. SnO_2-Sb* and *RuO_2*), which represent the state-of-the-art in the field of the electro-degradation of recalcitrant organics, effectively reduced the concentration of phenol to acceptable values, considering that the current provided to the cell was slightly more than the minimum required to achieve 100% of TOC reduction. The *SnO_2-Sb* sample reached a phenol conversion of 77.2% and a TOC reduction of 58.1%, which were the double of the values provided by the *Cat-MnO_x* electrode and four times the values obtained with the *An-MnO_x* sample. The high oxygen evolution overpotential attributed to this type of electrode is well-known in the literature [25,27,40–44], and is the main factor that allows antimony-doped tin oxide films to reach high efficiencies. In addition, the electrode based on *RuO_2* confirmed to be the best performing anode for phenol electro-degradation under atmospheric conditions, achieving a phenol conversion efficiency as high as 86.1% and a degree of mineralization equals to 66.4%. Such high efficiency of the ruthenium oxide film lies on its high activity and low overpotential towards a high number of electro-oxidation reactions, including water electrolysis [45,46], chlorine evolution [46,47] and organics abatement [24,29,48,49].

The *An-MnO_x* sample generated a lower and more stable cell potential (~5 V) than *Cat-MnO_x*, which instead started at 6 V and achieved 6.5 V at the end of the test (after 5 h). The working cell potential applied to the *SnO_2-Sb* electrode was of about 3.6 V and remains almost constant thorough the experiment, whereas the *RuO_2* anode provided the lowest and most stable potential (~2.7 V), due to the high stability of this noble-metal catalyst. These

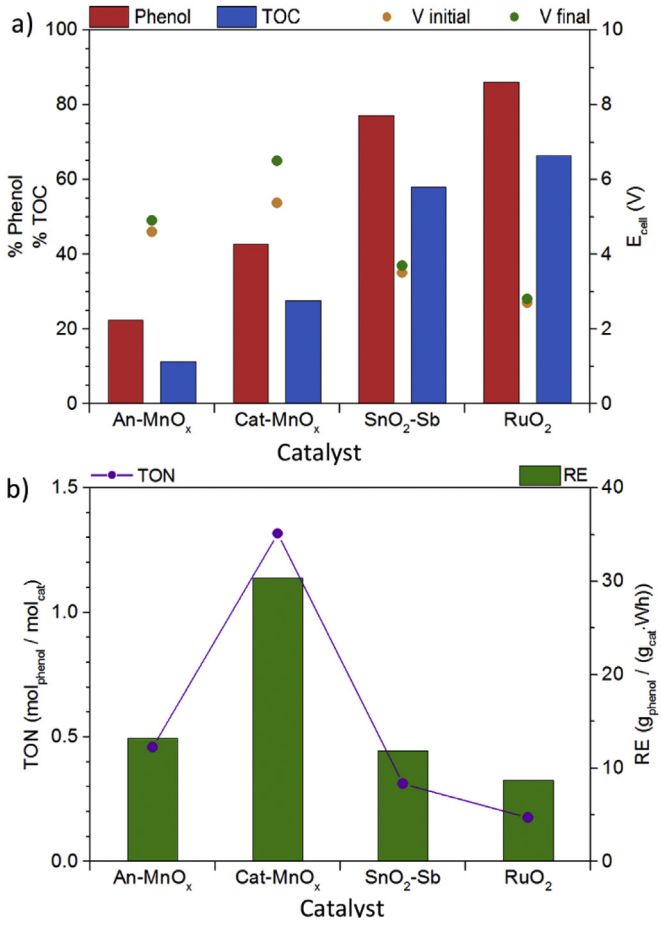

Fig. 4. (a) Phenol and TOC reduction, initial and final potentials and (b) Turn Over Number (TON) and Relative Efficiency (RE) for El-Ox tests carried out at ambient conditions and 2.5 mA/cm^2 for 5 h. Potentials are reported after ohmic drop compensation.

considerations were confirmed by the accelerated life-time tests, whose results are provided in Fig. S3 in the SI. The *Cat-MnO_x* sample was the least stable electrode, being deactivated after ~8 h, while the *An-MnO_x* sample demonstrated a service life of about 15 h. Instead, the state-of-the-art *SnO_2-Sb* material reached potential limit after about 25 h, whereas the *RuO_2* electrode maintained a constant potential for at least 30 h. These results indicate that further developments are still necessary to increase the stability of electrodeposited MnOx electrocatalysts.

However, the specific activities of the MnO_x-based electrodes were quite high and promising, as shown in Fig. 4b, although the phenol and TOC conversion obtained with the MnO_x electrodes were not complete. This is justified by the small amount of MnO_x deposited in the electrodes (*i.e.* 0.427 mgMn/cm^2 for the *An-MnO_x* sample and 0.285 mgMn/cm^2 for the *Cat-MnO_x*), which are one order of magnitude lower than the catalyst loading of the references electrodes (*i.e.* 2.170 mg_{Sn}/cm^2 for the *SnO_2-Sb* sample and 4.312 mg_{Ru}/cm^2 for the *RuO_2* sample). Therefore, both the Turn over numbers (TONs) and the relative efficiencies (REs) of the *Cat-MnO_x* sample were far higher than the ones obtained with the *SnO_2-Sb* and *RuO_2* electrodes, whereas the performances of the *An-MnO_x* sample were comparable to those of the reference catalysts, which was mainly due to the lower amount of material deposited on the Ti foil. In fact, the layer-by-layer electrodeposition of the *SnO_2-Sb* film required an overall deposition time of about 1 h, which is 6 times higher than the one required for the synthesis of the manganese oxide samples. The thermal brush-coating method used for the *RuO_2* deposited even more material on the surface of the titanium foil and the lack of control over the amount of deposited material is one of the principal drawbacks of that methods. For the previous reasons, other main advantages of the here proposed manganese oxide catalysts are the fast and low-cost electrodeposition technique used for their synthesis, their lower cost if compared to the ruthenium oxide and their lower toxicity if compared to antimony oxide material.

3.6. HTHP electro-oxidation tests

The thermal stability of phenol was assessed through two blank tests, both of those in which 1 l of phenol solution (100 mg/l) was put in the HTHP reactor compressed with N_2 up to 30 bar and heated up to 150 °C. After 5 h, the reactor was cooled and the pressure was released. In the first blank test, any purge was done before heating and compressing the system, while for the second blank test the system was purged with a N_2 flow for 1 h, to remove most of the dissolved oxygen from the solution. The effect of residual oxygen gas inside the starting solution (without N_2 purge) was far from being negligible, as it reduced the concentration of phenol to 8.6% and the TOC to 4.6% due to homogeneous catalytic pathways. Indeed, this phenomenon can be attributed to the reactivity of molecular oxygen towards organic molecules under the operative conditions similar to a Catalytic Wet Air Oxidation (CWAO) and to the residence time of the solution inside the reactor that was sufficient for the partial mineralization of phenol to CO_2 and H_2O. Instead, by purging the solution with N_2 before reaching the CWAO conditions, the degradation was limited to 2.3% and the mineralization was equal to 1.1%, most probably due to the lower oxidation and thermal degradation of phenol under those conditions. The results obtained with the different electrodes under different operative conditions in the HTHP reactor, after purging it from the atmospheric air, are reported in Fig. 5 and discussed in following.

3.6.1. Operative conditions (a): 85 °C, 30 bar and 10 mA/cm^2

The first tests in the HTHP reactor were made under operative conditions similar to a PEM electrolyzer: 85 °C and 30 bar, with an applied current density of 10 mA/cm^2 for a reaction time of 2 h. From Fig. 5a it is evident that the degradation efficiency of the *An-MnO_x* sample was improved with respect to the ambient conditions, since the phenol conversion resulted to be more than doubled at 85 °C and 30 bar, reaching values of phenol and TOC conversion of 55.6% and 43.9%, respectively. Those valued were even higher than the ones obtained by the *Cat-MnO_x* sample, which achieved a phenol and TOC degradation of about 48.3% and 35.7%, respectively, and did not increased its efficiency with respect to the ambient El-Ox test. This behavior could be attributed to the higher tendency of the α-Mn_2O_3 phase (mainly present in the anodic electrodeposited film, *An-MnO_x*) to oxidize water to O_2, that would be rapidly released to the gaseous phase under ambient pressure conditions, while it might remain dissolved in a higher extend at 30 bar, thus being more reactive at high temperatures and high pressures.

By using the two reference anodes: *SnO_2-Sb* and *RuO_2*, only a slight increase in the phenol conversion efficiency was reported: 82.3% for the *SnO_2-Sb* and 88.9% for the *RuO_2*. However, the TOC reduction was noticeably enhanced (by at least 20%), proving the beneficial effect of rising temperature and pressure, which contributed to obtain a higher degree of mineralization of the phenol-containing wastewater.

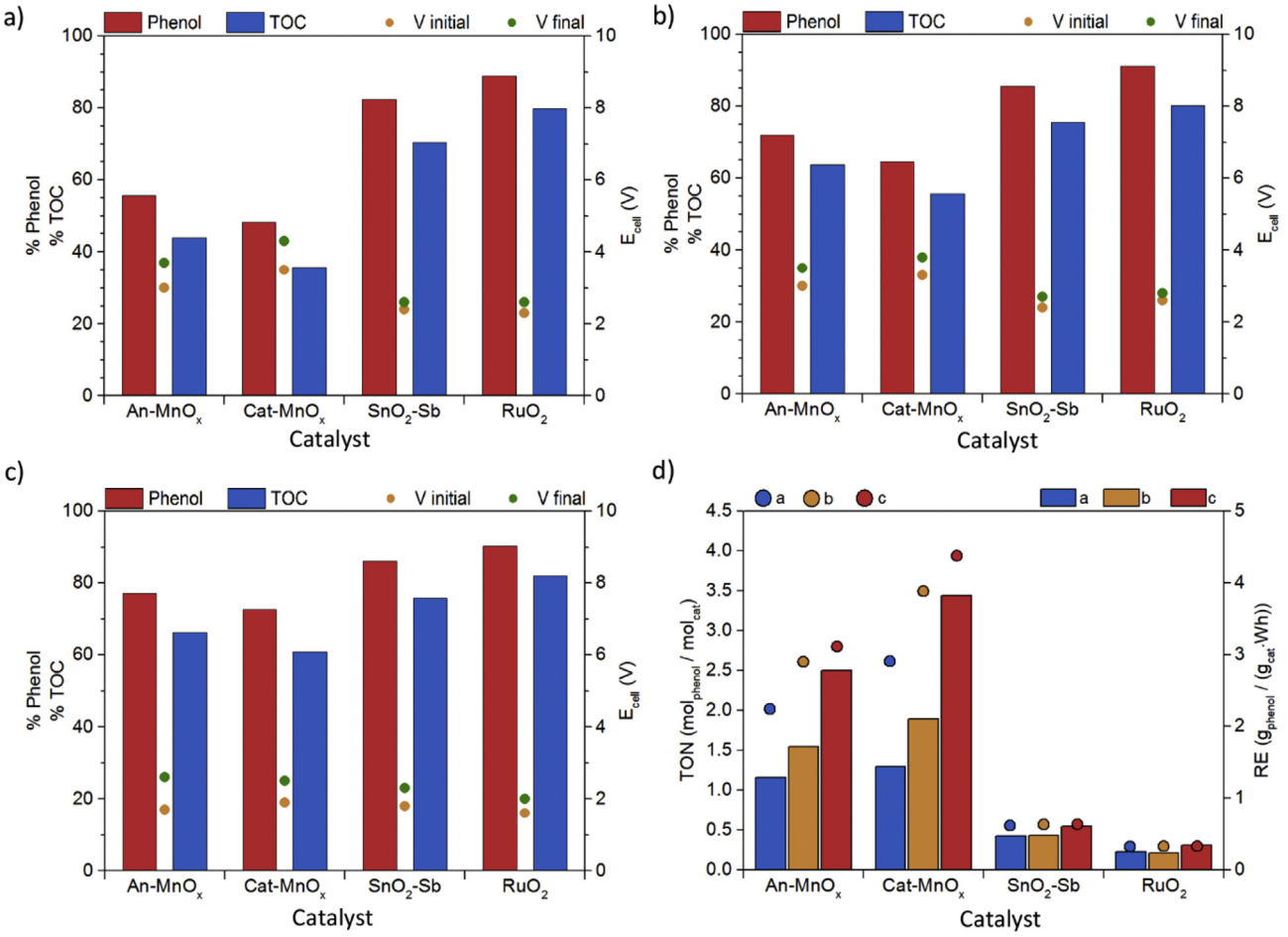

Fig. 5. Phenol and TOC reduction, initial and final potentials for El-Ox tests carried out at: (a) 85 °C, 30 bar at 400 mA for 2 h; (b) 85 °C, 30 bar at 200 mA for 4 h; (c) 150 °C, 30 bar at 800 mA for 1 h. Potentials are reported after ohmic drop compensation. (d) Turn over number (TON, dots) and Relative Efficiency (RE, bars) under the conditions reported in (a), (b) and (c), respectively.

3.6.2. Operative conditions (b): 85 °C, 30 bar and 5 mA/cm^2

Another test was carried out at 85 °C and 30 bar, but with a lower current density (*i.e.* 5 mA/cm^2) and a higher reaction time (*i.e.* 4 h) than the previous conditions (a), thus, leaving unvaried the total amount of charge needed to completely degrade the phenol in the solution. In this way, the effect of current and time on the efficiency of the process was analyzed.

As expected, a halved current density with a doubled residence time resulted in enlarged faradaic efficiencies, as noticed from the increased TOC reduction for all the samples. This improvement could be attributed to the reduction of irreversibilities, such as ohmic drop, polarization and mass transfer limitations, which usually occurred at higher current densities. Moreover, the improved exploitation of the O_2 evolved at the anode could be an additional explanation for this trend. In fact, if the applied current density is too high, the oxygen formed at the surface of the electrode develops too quickly to react with the organic molecules, as the mass transfer of phenol from the bulk of the solution becomes the limiting factor. Therefore, not all the O_2 electro-generated is used for electro-degradation but could be released as gas bubbles.

3.6.3. Operative conditions (c): 150 °C, 30 bar and 20 mA/cm^2

The second set of tests in HTHP conditions was conducted at 150 °C and 30 bar. In the first experiment, a current density of 20 mA/cm^2 was applied to the system for 1 h and the outputs are shown in Fig. 5c. If compared to the tests at 85 °C, the performance of all the electrodes, especially those of the MnO_x electrodes, were visibly improved. This high effectiveness, despite the demanding operative conditions, was probably due to the CWAO conditions, so the O_2 reactivity towards the degradation of phenol was boosted and it prevailed over the irreversibilities and the mass transfer limitations described before. Moreover, the working potential of the system was kept at limited values (after ohmic drop compensation), even though the applied current was elevated, proving the beneficial effect of the temperature on the electro-oxidation process. Under these conditions, the overall performance of both *An-MnO_x* and *Cat-MnO_x* electrodes was similar to the one offered by the *SnO_2-Sb* and *RuO_2* reference anodes, thus encouraging the application of these materials for the electro-oxidation of recalcitrant organics.

To assess the O_2 evolution performances of the anodes, linear sweep voltammetries (LSV) were carried out in 0.1 M Na_2SO_4 solution, at a scan rate of 5 mV/s. The oxygen evolution reaction (OER) potential was conventionally measured at a current density of 0.1 mA/cm^2 [15]. As shown in Fig. S4 in the SI, the *RuO_2* sample demonstrated the lowest OER potential (of about 1.92 V vs. RHE), while the *SnO_2-Sb* material gave the highest value, of about 2.4 V vs. RHE. These results were expected, as *RuO_2* is a well-known catalyst for water electrolysis, while *SnO_2-Sb* is effectively employed for organics degradation. The *An-MnO_x* electrode (*i.e.* Mn^{3+}) presented an OER potential of about 2.15 V vs. RHE, followed by *Cat-MnO_x* (*i.e.* Mn^{4+}), with an OER potential of 2.30 V vs. RHE, in accordance with

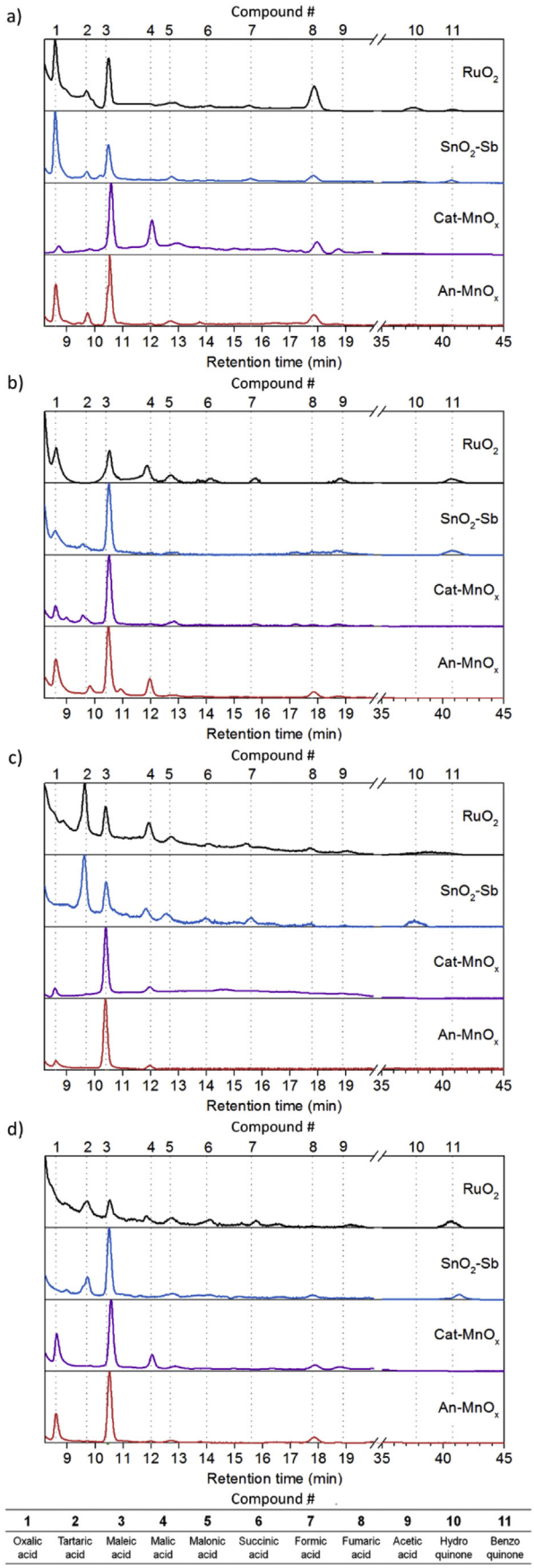

Fig. 6. HPLC chromatograms for El-Ox tests carried out at (a) ambient conditions at 2.5 mA for 5 h, (b) 85 °C, 30 at 400 mA for 2 h, (c) 85 °C, 30 at 200 mA for 4 h and (d) 150 °C, 30 at 800 mA for 1 h.

previous literature reports [15,36,37,50].

3.6.4. Turn over number (TON) and relative efficiency (RE)

The last comparison between the HTHP tests was made by analyzing the TONs and REs of the coated electrodes. The TON referred to the metal (e.g. Mn) active sites was calculated as the moles of phenol degraded divided by the moles of metal in the electrodes [18]. In the same manner, the RE related to the energy consumption was calculated by dividing the TON by the total applied energy (in Wh) provided to the electrode during the degradation test [18]. In this case, the amount of catalyst material deposited in the electrodes (which was measured by using a microbalance) were: 0.403 mg/cm^2 of *An-MnO$_x$*, 0.270 mg/cm^2 of *Cat-MnO$_x$*, 2.178 mg/cm^2 of *SnO$_2$-Sb* and 4.511 mg/cm^2 of *RuO$_2$*. As can be seen in Fig. 5d, the TONs of both MnO_x electrodes are much higher than the ones obtained with the reference catalysts: the *An-MnO$_x$* sample gave a TON that was about 5 times higher than the *SnO$_2$-Sb* sample and about 10 times higher than the *RuO$_2$ electrode*, whereas the *Cat-MnO$_x$* sample provided a TON about 7 and 12 times greater than the *SnO$_2$-Sb* and *RuO$_2$* samples, respectively.

The relative efficiencies (REs) followed the same trend of the TONs: the MnO_x electrodes achieved a higher RE than the reference materials. However, each electrode had a different behavior in function of the experimental conditions, as the REs depends also on the energy provided to the system, which is related to: the applied current density, cell potential and reaction time. Therefore, it is useful to analyze the influence of the operative conditions on the effectiveness of the process.

Changes in the operative conditions strongly influenced the RE of the MnO_x electrodes. When moving towards CWAO ranges or to slower reaction rates, the application of lower current densities (and cell potentials) as well as the reduction of the reaction time, in turns decreased the energy provided to the system and increased the relative efficiency. This trend was less noticeable for the reference anodes, since the original conversions were already high and the HTHP reactions did not noticeably affect their performances.

3.7. Analysis of the reaction mechanism

Since few works exist on the electro-oxidation of phenol on manganese oxide electrodes and, to the best of the authors' knowledge, no works concerning the El-Ox of phenol under HTHP conditions have been carried out; we have investigated the intermediates produced during the reaction, to gain insights on the reaction mechanism of the phenol degradation over MnO_x.

Fig. 6 reports the HPLC chromatograms for the anodes tested at ambient conditions (a), at PEM electrolysis conditions and either high (b) or low (c) current densities, and at CWAO conditions (d). Based on the by-products found in the solutions, a degradation pathway is proposed as reported in Fig. 7. From a comparison between the MnO_x-based films and the reference anodes (*i.e. SnO$_2$-Sb* and *RuO$_2$*) it was evident the presence of benzoquinone and hydroquinone in the solutions treated with the latter two electrodes. Benzoquinone ($t_R = 40.8$ min) and hydroquinone ($t_R = 37.9$ min) form a redox couple that is found when the electrochemical cell is undivided. This is commonly recognized as the first step in the electrochemical degradation of phenol (see top of Fig. 7), after the formation of phenoxy radicals, which are also the responsible for possible fouling of the electrodes when reacting with quinones to form insoluble polymeric compounds [32,42,51–53]. Their peaks are clearly distinguishable from the other intermediates, which are all carboxylic and dicarboxylic acids, as their retention times are noticeably higher under the adopted chromatographic conditions. The absence of these compounds when using the *An-MnO$_x$* and *Cat-MnO$_x$* electrodes demonstrated that, probably, the aromatic ring

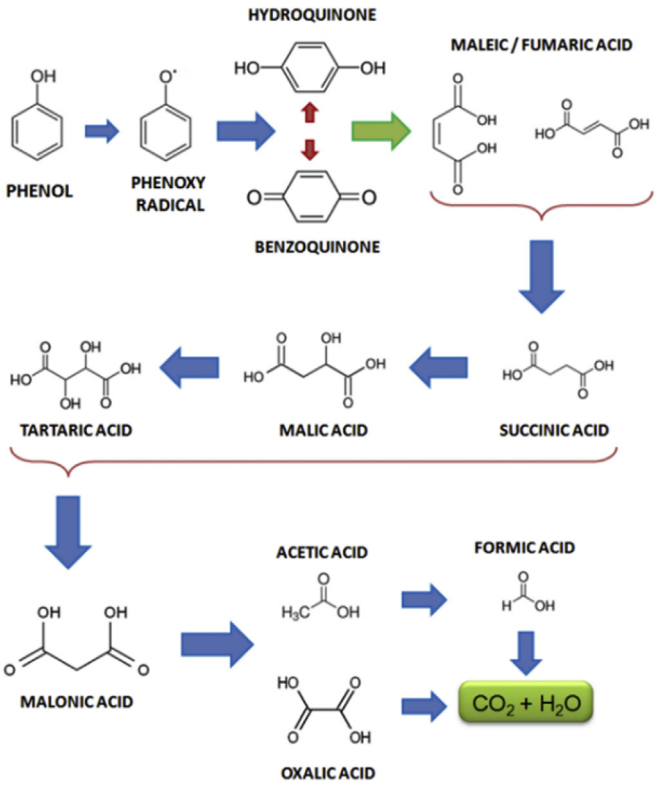

Fig. 7. Proposed degradation pathways during phenol Electro-oxidation.

opening from quinones to maleic acid ($t_R = 10.4$ min) and its *trans* isomer fumaric acid ($t_R = 17.8$ min) was not a limiting step, unlike for the *SnO₂-Sb* and *RuO₂* anodes. This step has been reported in previous works as a key reaction limiting the overall phenol mineralization [51,53].

Other low molecular weight intermediates were identified, for almost all the final solutions. Succinic acid ($t_R = 14.0$ min) [32,53] is commonly derived from the reduction of the couple maleic/fumaric acid [32], which could happen at the cathode. Further oxidation could occur, with the formation of malic acid ($t_R = 12.0$ min) [52,53], which can also be obtained by direct hydration of maleic/fumaric acid, and then tartaric acid ($t_R = 9.7$ min) [52]. All these acids, constituted by four carbons, can be transformed into the three-carbon malonic acid ($t_R = 12.7$ min) [32,51,52]. From malonic acid two different intermediates can be obtained: oxalic acid ($t_R = 8.6$ min) [32,42,51–53] and acetic acid ($t_R = 18.9$ min) [32,51]. The first one is the lowest molecular weight dicarboxylic acid, which in turn could be completely mineralized; the second one, can be firstly degraded to formic acid ($t_R = 15.6$ min) [51,53], and then be converted to CO_2 and water.

Also, the influence of the operative conditions was analyzed. It is possible to state that the experiments at high temperature did not modify the reaction mechanism, but they improved the conversion towards lower molecular weight products and, ultimately, into CO_2 and H_2O. In fact, many of the peaks related to fumaric, malonic and malic acid, and partially of oxalic acid, decreased their intensity by increasing the temperature. Under CWAO operative conditions, the only noticeable intermediate was maleic acid, however, this was also due to its higher absorption coefficient in comparison to other compounds at the UV wavelength (~206 nm) used for the HPLC analyses.

4. Conclusions

Two types of MnO_x-based electrocatalysts were synthesized on titanium foil by anodic or cathodic electrodeposition methods, obtaining mixed α-Mn_2O_3 + α-MnO_2 phases or α-MnO_2, respectively, and they were tested for the elctro-oxidation of phenol. At ambient conditions, the *An-MnO$_x$* sample showed a poor phenol conversion (~22%), while the *Cat-MnO$_x$* electrode proved a moderate activity (~43%) in comparison with the *SnO₂-Sb* and the *RuO₂* state-of-the-art anodes that achieved, as expected, better activities, *i.e.* ~77% and ~86% of phenol conversion, respectively. After a screening of different operative conditions of pressure (30 bar), temperature (85 °C and 150 °C) and current densities (5, 10 and 20 mA/cm^2), we found that under mild catalytic wet air oxidation conditions (*i.e.* 150 °C and 30 bar) the both the *An-MnO$_x$* and *Cat-MnO$_x$* samples achieved conversion efficiencies (~77% and 72%, respectively) comparable to those of the state-of-the-art reference anodes: *SnO₂-Sb* and *RuO₂*, which instead did not improved their performances by increasing temperature and pressure in the system. In addition, lower current densities caused a positive effect in the phenol conversion, most probably due to reduced overpotentials in the reaction system. The here presented results demonstrated that the electro-generated oxygen, easily formed during the water splitting reaction by the α-Mn_2O_3 phase that constitutes the *An-MnOx* sample, represents a highly reactive specie that can be exploited under mild pressure and temperature conditions for the degradation of recalcitrant organics. In addition, the increase of temperature contributed to improve kinetics and to reduce reaction overpotentials, while a high pressure enhanced the oxygen dissolution allowing its exploitation for phenol degradation. The HPLC analysis of the treated solutions evidenced traces of many by-products, which are commonly observed in literature, such as quinones, or bicarboxylic acids, demonstrating that the reaction mechanism is not significantly influenced by temperature and pressure.

It is worth of notice that the turn over number and relative efficiency of both MnO_x materials were from 2 to 12 times higher than those of the state-of-the-art catalysts, under the here investigated HTHP conditions. However, although the here proposed approach is very promising, further developments on the MnO_x-based electrodes are required to increase their stability for a practical implementation as substitutes of noble-metal based electrocatalysts. Future developments could also concern the study of more complex wastewater matrixes, containing also biodegradable compounds (e.g. glucose) or nitrogenous molecules (e.g. urea). Besides, due to favored thermodynamics and kinetics of the here proposed HTHP electrochemical approach, a proper tuning of the operative conditions (*i.e.* residence time in the electrochemical reactor) could be exploited for the synthesis of high added-value products from the electrochemical treatment of organic compounds in wastewaters.

Acknowledgments

This work has been funded by the EU Framework Program Horizon 2020: Project TERRA, Grant agreement number 677471 and Project CELBICON, Grant agreement number 679050. The authors would like also to thank Mauro Raimondo for FESEM analysis, Camilla Galletti and Fabio Deorsola for XRD analysis.

Appendix B. Supplementary data

Supplementary data related to this article can be found at https://doi.org/10.1016/j.electacta.2018.03.178.

References

[1] R. Maciel, G.L. Sant'Anna Jr., M. Dezotti, Phenol removal from high salinity effluents using Fenton's reagent and photo-Fenton reactions, Chemosphere 57 (2004) 711–719.

[2] K. Turhan, S. Uzman, Removal of phenol from water using ozone, Desalination 229 (2008) 257–263.

[3] F. Stüber, J. Font, A. Eftaxias, M. Paradowska, M.E. Suarez, A. Fortuny, C. Bengoa, A. Fabregat, Chemical wet oxidation for the abatement of refractory non-biodegradable organic wastewater pollutants, Process Saf. Environ. Protect. 83 (2005) 371–380.

[4] F. Martínez, J.A. Melero, J.Á. Botas, M.I. Pariente, R. Molina, Treatment of phenolic effluents by catalytic wet hydrogen peroxide oxidation over Fe2O3/SBA-15 extruded catalyst in a fixed-bed reactor, Ind. Eng. Chem. Res. 46 (2007) 4396–4405.

[5] G. Busca, S. Berardinelli, C. Resini, L. Arrighi, Technologies for the removal of phenol from fluid streams: a short review of recent developments, J. Hazard. Mater. 160 (2008) 265–288.

[6] W. Yun-Hai, C. Qing-Yun, L. Guo, L. Xiang-Lin, Anodic Materials with High Energy Efficiency for Electrochemical Oxidation of Toxic Organics in Waste Water, INTECH Open Access Publisher, 2012.

[7] Á. Anglada, A. Urtiaga, I. Ortiz, Contributions of electrochemical oxidation to waste-water treatment: fundamentals and review of applications, J. Chem. Technol. Biotechnol. 84 (2009) 1747–1755.

[8] K.-H. Kim, S.-K. Ihm, Heterogeneous catalytic wet air oxidation of refractory organic pollutants in industrial wastewaters: a review, J. Hazard. Mater. 186 (2011) 16–34.

[9] S.-W. Lee, C.-W. Lee, S.-B. Yoon, M.-S. Kim, J.H. Jeong, K.-W. Nam, K.C. Roh, K.-B. Kim, Superior electrochemical properties of manganese dioxide/reduced graphene oxide nanocomposites as anode materials for high-performance lithium ion batteries, J. Power Sources 312 (2016) 207–215.

[10] M. Sawangphruk, P. Srimuk, P. Chiochan, A. Krittayavathananon, S. Luanwuthi, J. Limtrakul, High-performance supercapacitor of manganese oxide/reduced graphene oxide nanocomposite coated on flexible carbon fiber paper, Carbon 60 (2013) 109–116.

[11] J. Jiang, A. Kucernak, Electrochemical supercapacitor material based on manganese oxide: preparation and characterization, Electrochim. Acta 47 (2002) 2381–2386.

[12] A. Rafique, A. Massa, M. Fontana, S. Bianco, A. Chiodoni, C.F. Pirri, S. Hernández, A. Lamberti, Highly uniform anodically deposited film of MnO2 nanoflakes on carbon fibers for flexible and wearable fiber-shaped supercapacitors, ACS Appl. Mater. Interfaces 9 (2017) 28386–28393.

[13] C. Ottone, M. Armandi, S. Hernández, S. Bensaid, M. Fontana, C.F. Pirri, G. Saracco, E. Garrone, B. Bonelli, Effect of surface area on the rate of photocatalytic water oxidation as promoted by different manganese oxides, Chem. Eng. J. 278 (2015) 36–45.

[14] F. Zhou, A. Izgorodin, R.K. Hocking, L. Spiccia, D.R. MacFarlane, Electrodeposited MnOx films from ionic liquid for electrocatalytic water oxidation, Adv. En. Mater. 2 (2012) 1013–1021.

[15] A. Ramírez, P. Hillebrand, D. Stellmach, M.M. May, P. Bogdanoff, S. Fiechter, Evaluation of MnOx, Mn2O3, and Mn3O4 electrodeposited films for the oxygen evolution reaction of water, J. Phys. Chem. C 118 (2014) 14073–14081.

[16] T. Yousefi, A.N. Golikand, M.H. Mashhadizadeh, M. Aghazadeh, Hausmannite nanorods prepared by electrodeposition from nitrate medium via electrogeneration of base, J. Taiwan Ins. Chem. Eng. 43 (2012) 614–618.

[17] G. Sotgiu, M. Foderà, F. Marra, E. Petrucci, Production and characterization of manganese oxide-based electrodes for anodic oxidation of organic compounds, Chem. Eng. Trans. 41 (2014) 115–120.

[18] A. Massa, S. Hernández, A. Lamberti, C. Galletti, N. Russo, D. Fino, Electrooxidation of phenol over electrodeposited MnOx nanostructures and the role of a TiO2 nanotubes interlayer, Appl. Catal. B 203 (2017) 270–281.

[19] F. Allebrod, C. Chatzichristodoulou, M.B. Mogensen, Alkaline electrolysis cell at high temperature and pressure of 250 C and 42 bar, J. Power Sources 229 (2013) 22–31.

[20] J.C. Ganley, High temperature and pressure alkaline electrolysis, Int. J. Hydrogen Energy 34 (2009) 3604–3611.

[21] B. Laoun, Thermodynamics aspect of high pressure hydrogen production by water electrolysis, Revue des energies renouvelables 10 (2007) 435–444.

[22] D. Todd, M. Schwager, W. Mérida, Thermodynamics of high-temperature, high-pressure water electrolysis, J. Power Sources 269 (2014) 424–429.

[23] F. Marangio, M. Santarelli, M. Calì, Theoretical model and experimental analysis of a high pressure PEM water electrolyser for hydrogen production, Int. J. Hydrogen Energy 34 (2009) 1143–1158.

[24] I.D.d. Santos, J.C. Afonso, A.J.B. Dutra, Electrooxidation of Phenol on a Ti/RuO2 anode: effect of some electrolysis parameters, J. Braz. Chem. Soc. 22 (2011) 875–883.

[25] C.-S. SHIN, S.-i. MHO, Electrocatalytic oxidation of phenol and its derivatives at Sb 5+ doped SnO 2 electrodes, Anal. Sci. Suppl. 17 (2002) a65–a68.

[26] X. Chen, F. Gao, G. Chen, Comparison of Ti/BDD and Ti/SnO2–Sb2O5 electrodes for pollutant oxidation, J. Appl. Electrochem. 35 (2005) 185–191.

[27] L. Lipp, D. Pletcher, The preparation and characterization of tin dioxide coated titanium electrodes, Electrochim. Acta 42 (1997) 1091–1099.

[28] Y. Chen, L. Hong, H. Xue, W. Han, L. Wang, X. Sun, J. Li, Preparation and characterization of TiO 2-NTs/SnO 2-Sb electrodes by electrodeposition, J. Electroanal. Chem. 648 (2010) 119–127.

[29] A.R. de Andrade, P.M. Donate, P.P. Alves, C.H. Fidellis, J.F. Boodts, Ethanol electro-oxidation in ruthenium-oxide-coated titanium electrodes, J. Electrochem. Soc. 145 (1998) 3839–3843.

[30] M. Carmo, D.L. Fritz, J. Mergel, D. Stolten, A comprehensive review on PEM water electrolysis, Int. J. Hydrogen Energy 38 (2013) 4901–4934.

[31] J. Levec, A. Pintar, Catalytic wet-air oxidation processes: a review, Catal. Today 124 (2007) 172–184.

[32] X.-y. Li, Y.-h. Cui, Y.-j. Feng, Z.-m. Xie, J.-D. Gu, Reaction pathways and mechanisms of the electrochemical degradation of phenol on different electrodes, Water Res. 39 (2005) 1972–1981.

[33] M.C. Biesinger, B.P. Payne, A.P. Grosvenor, L.W. Lau, A.R. Gerson, R.S.C. Smart, Resolving surface chemical states in XPS analysis of first row transition metals, oxides and hydroxides: Cr, Mn, Fe, Co and Ni, Appl. Surf. Sci. 257 (2011) 2717–2730.

[34] R. Horne, G. Frysinger, The effect of pressure on the electrical conductivity of sea water, J. Geophys. Res. 68 (1963) 1967–1973.

[35] T. Takashima, K. Hashimoto, R. Nakamura, Inhibition of charge disproportionation of MnO2 electrocatalysts for efficient water oxidation under neutral conditions, J. Am. Chem. Soc. 134 (2012) 18153–18156.

[36] T. Takashima, K. Hashimoto, R. Nakamura, Mechanisms of pH-dependent activity for water oxidation to molecular oxygen by MnO2 electrocatalysts, J. Am. Chem. Soc. 134 (2012) 1519–1527.

[37] S. Hernández, C. Ottone, S. Varetti, M. Fontana, D. Pugliese, G. Saracco, B. Bonelli, M. Armandi, Spin-coated vs. Electrodeposited Mn oxide films as water oxidation catalysts, Materials 9 (2016) 296.

[38] G.V. Sokol'skii, S.V. Ivanova, N.D. Ivanova, E.I. Boldyrev, T.F. Lobunets, T.V. Tomila, Doped manganese (IV) oxide in processes of destruction and removal of organic compounds from aqueous solutions, J. Water Chem. Technol. 34 (2012) 227–233.

[39] W.-c. Peng, S.-b. Wang, X.-y. Li, Shape-controlled synthesis of one-dimensional α-MnO2 nanocrystals for organic detection and pollutant degradation, Separ. Purif. Technol. 163 (2016) 15–22.

[40] B. Correa-Lozano, C. Comninellis, A. De Battisti, Service life of Ti/SnO2–Sb2O5 anodes, J. Appl. Electrochem. 27 (1997) 970–974.

[41] H.-y. Ding, Y.-j. Feng, J.-f. Liu, Preparation and properties of Ti/SnO 2–Sb 2 O 5 electrodes by electrodeposition, Mater. Lett. 61 (2007) 4920–4923.

[42] D. He, S.-i. Mho, Electrocatalytic reactions of phenolic compounds at ferric ion co-doped SnO 2: Sb 5+ electrodes, J. Electroanal. Chem. 568 (2004) 19–27.

[43] J.-t. KONG, S.-y. SHI, X.-p. ZHU, J.-r. NI, Effect of Sb dopant amount on the structure and electrocatalytic capability of Ti/Sb-SnO 2 electrodes in the oxidation of 4-chlorophenol, J. Environ. Sci. 19 (2007) 1380–1386.

[44] A.M. Polcaro, S. Palmas, F. Renoldi, M. Mascia, On the performance of Ti/SnO2 and Ti/PbO2 anodesin electrochemical degradation of 2-chlorophenolfor wastewater treatment, J. Appl. Electrochem. 29 (1999) 147–151.

[45] H. Ma, C. Liu, J. Liao, Y. Su, X. Xue, W. Xing, Study of ruthenium oxide catalyst for electrocatalytic performance in oxygen evolution, J. Mol. Catal. A Chem. 247 (2006) 7–13.

[46] T. Arikawa, Y. Murakami, Y. Takasu, Simultaneous determination of chlorine and oxygen evolving at RuO2/Ti and RuO2–TiO2/Ti anodes by differential electrochemical mass spectroscopy, J. Appl. Electrochem. 28 (1998) 511–516.

[47] V. Panic, A. Dekanski, S. Milonjic, V.B. Miskovic-Stankovic, B. Nikolic, Activity and stability of RuO~ 2 coated titanium anodes prepared via the alkoxide route, J. Serb. Chem. Soc. 71 (2006) 1173–1185.

[48] Y. Yavuz, A.S. Koparal, Electrochemical oxidation of phenol in a parallel plate reactor using ruthenium mixed metal oxide electrode, J. Hazard Mater. 136 (2006) 296–302.

[49] M. Li, C. Feng, W. Hu, Z. Zhang, N. Sugiura, Electrochemical degradation of phenol using electrodes of Ti/RuO2–Pt and Ti/IrO2–Pt, J. Hazard. Mater. 162 (2009) 455–462.

[50] A. Ramírez, D. Friedrich, M. Kunst, S. Fiechter, Charge carrier kinetics in MnOx, Mn2O3 and Mn3O4 films for water oxidation, Chem. Phys. Lett. 568–569 (2013) 157–160.

[51] N.D. Mu'azu, M.H. Al-Malack, Influence of some operating parameters on electro-oxidation of phenol using boron doped diamond anode and graphite cathode, J. Environ. Sci. Tech. 5 (2012) 460.

[52] P.D. Alves, M. Spagnol, G. Tremiliosi-Filho, A.R.d. Andrade, Investigation of the influence of the anode composition of DSA-type electrodes on the electrocatalytic oxidation of phenol in neutral medium, J. Braz. Chem. Soc. 15 (2004) 525–533.

[53] M. Pimentel, Oxidation of Phenol and Cresol by Electrochemical Advanced Oxidation Method in Homogeneous Medium: Application to Treatment of a Real Effluent of Aeronautical Industry, Université Paris-Est, 2008.